

## Durham Research Online

---

### Deposited in DRO:

10 April 2018

### Version of attached file:

Accepted Version

### Peer-review status of attached file:

Peer-reviewed

### Citation for published item:

Cormier, Marc-André and Werner, Roland A. and Sauer, Peter E. and Gröcke, Darren R. and Leuenberger, Markus C. and Wieloch, Thomas and Schleucher, Jürgen and Kahmen, Ansgar (2018) '2Hfractionations during the biosynthesis of carbohydrates and lipids imprint a metabolic signal on the 2H values of plant organic compounds.', *New phytologist*, 218 (2). pp. 479-491.

### Further information on publisher's website:

<https://doi.org/10.1111/nph.15016>

### Publisher's copyright statement:

This is the accepted version of the following article: Cormier, Marc-André, Werner, Roland A., Sauer, Peter E., Gröcke, Darren R., Leuenberger, Markus C., Wieloch, Thomas, Schleucher, Jürgen Kahmen, Ansgar (2018). 2Hfractionations during the biosynthesis of carbohydrates and lipids imprint a metabolic signal on the 2H values of plant organic compounds. *New Phytologist* 218(2): 479-491 which has been published in final form at <https://doi.org/10.1111/nph.15016>. This article may be used for non-commercial purposes in accordance With Wiley Terms and Conditions for self-archiving.

### Additional information:

## Use policy

---

The full-text may be used and/or reproduced, and given to third parties in any format or medium, without prior permission or charge, for personal research or study, educational, or not-for-profit purposes provided that:

- a full bibliographic reference is made to the original source
- a [link](#) is made to the metadata record in DRO
- the full-text is not changed in any way

The full-text must not be sold in any format or medium without the formal permission of the copyright holders.

Please consult the [full DRO policy](#) for further details.

1 Title:  $^2\text{H}$ -fractionations during the biosynthesis of carbohydrates and lipids imprint a  
2 metabolic signal on the  $\delta^2\text{H}$  values of plant organic compounds

3  
4 Authors: Cormier M-A.<sup>a,b,\*</sup>, Werner R. A.<sup>a</sup>, Sauer P. E.<sup>c</sup>, Gröcke D. R.<sup>d</sup>, Leuenberger  
5 M. C.<sup>e</sup>, Wieloch T.<sup>f</sup>, Schleucher J.<sup>f</sup> and Kahmen A.<sup>b</sup>

6  
7 Affiliations:

8 <sup>a</sup>ETH Zürich, Department of Environmental Systems Science,  
9 Universitätstrasse 2, 8092 Zürich, Switzerland.

10 <sup>b</sup>University of Basel, Department of Environmental Sciences - Botany,  
11 Schönbeinstrasse 6, 4056 Basel, Switzerland.

12 <sup>c</sup>Department of Geological Sciences, Indiana University, Bloomington, IN  
13 47405-1405, USA.

14 <sup>d</sup>Stable Isotope Biogeochemistry Laboratory, Durham University, Science  
15 Laboratories, South Road, Durham, DH1 3LE, UK.

16 <sup>e</sup>Climate and Environmental Physics, Physics Institute and Oeschger Centre for  
17 Climate Change Research, University of Bern, Bern, Switzerland

18 <sup>f</sup>Department of Medical Biochemistry and Biophysics, Umeå University, 901  
19 87 Umeå, Sweden.

20 \*Corresponding author: [marc-andre.cormier@usys.ethz.ch](mailto:marc-andre.cormier@usys.ethz.ch)

21  
22 Keywords: alkanes, cellulose, biomarker, hydrogen isotopes, plant metabolism

## Abstract

- $\delta^2\text{H}$  analyses of plant organic compounds have been applied to assess ecohydrological processes in the environment despite a large part of the  $\delta^2\text{H}$  variability observed in plant compounds not being fully elucidated.
- We present a new conceptual biochemical model based on empirical H isotope data that we generated in two complementary experiments that explains where  $^2\text{H}$ -fractionations occur in the biosynthesis of plant organic compounds and how these  $^2\text{H}$ -fractionations are tightly coupled to a plant's carbon and energy metabolism.
- With this work, we demonstrate that information recorded in the  $\delta^2\text{H}$  values of plant organic compounds goes beyond hydrological signals and can also contain important information on the carbon and energy metabolism of plants. As such we provide a mechanistic basis to introduce hydrogen isotopes in plant organic compounds as new metabolic proxy for the carbon and energy metabolism of plants and ecosystems. Such a new metabolic proxy has the potential to be applied in a broad range of disciplines, including plant and ecosystem physiology, biogeochemistry and paleoecology.

## Introduction

The analyses of stable isotope ratios in plant material have proven to be an indispensable tool for ecological, biogeochemical and (paleo-) climatological research (Dawson et al., 2002). Of the four most common biogenic elements, only carbon (C), oxygen (O), and nitrogen (N) isotope ratios of plant compounds are fully established as proxies for different ecological, environmental and paleoclimatological processes. In contrast, hydrogen (H) isotope ratios in plant compounds are less commonly applied. New developments in isotope-ratio mass spectrometry for compound-specific analyses (Burgoyne & Hayes, 1998), e.g. of leaf wax lipids, and new equilibration methods (Filot et al., 2006) have, however, promoted the use of H isotopes in recent years. In particular, H isotope analyses of biomarkers such as leaf waxes have been successfully applied in paleohydrological research over the past decade and have highlighted the tremendous potential of hydrogen isotope ratios in plant-derived compounds for ecological, environmental and paleoclimatological research (Sachse et al., 2012).

Three main drivers that have been identified to determine the H isotope composition ( $\delta^2\text{H}$ ) in plant organic compounds are: (i)  $\delta^2\text{H}$  of the plant's water source (Chikaraishi & Naraoka, 2003; Sachse *et al.*, 2006; Hou *et al.*, 2008), (ii) leaf water evaporative  $^2\text{H}$ -enrichment, which is largely driven by the evaporative environment of the plant (Smith & Freeman, 2006; Feakins & Sessions, 2010a; Kahmen *et al.*, 2013a,b), and (iii) biosynthetic  $^2\text{H}$ -fractionation ( $^2\text{H}\text{-}\epsilon_{\text{bio}}$ ), which includes several different biochemical processes and corresponds to the  $^2\text{H}$ -fractionation between the biosynthetic cellular water pool and the organic compounds (Ziegler *et al.*, 1976; Sternberg *et al.*, 1984b; Ziegler, 1989; Yakir & DeNiro, 1990; Luo & Sternberg, 1992; Yakir, 1992; Schmidt *et al.*, 2003).

Most biogeochemical and paleohydrological studies that have applied stable H isotopes in plant-derived biomarkers have considered  $^2\text{H}\text{-}\epsilon_{\text{bio}}$  for any given compound to be constant within a species (e.g. Sachse *et al.*, 2004; 2006). As such,  $\delta^2\text{H}$  values in plant organic compounds are assumed to be mainly influenced by the plant's source water  $\delta^2\text{H}$  values and the evaporative  $^2\text{H}$ -enrichment of leaf water (i.e. Rach et al., 2014). The  $\delta^2\text{H}$  values of e.g. leaf wax *n*-alkanes are thus increasingly applied as proxy for (paleo-) hydrological processes (Sachse et al., 2012). However, there are indications that  $^2\text{H}$ -

$\epsilon_{\text{bio}}$  can vary for a given compound within a species and that this variability is related to the C metabolism of the plant (Ziegler *et al.*, 1976; Estep & Hoering, 1980; Yakir & DeNiro, 1990; Luo & Sternberg, 1992; Schmidt *et al.*, 2003; Liu & Huang, 2008; Pedentchouk *et al.*, 2008). It has been suggested that photosynthetic H isotope fractionation processes during the reduction of NADPH in the light reaction of photosynthesis and the primary assimilation of triose phosphates, and particularly post-photosynthetic  $^2\text{H}$ -fractionation processes, which correspond to all other reactions following this primary assimilation, determine  $^2\text{H}$ - $\epsilon_{\text{bio}}$  in plants (Roden *et al.*, 2000). A comprehensive understanding of how variations in photosynthetic and post-photosynthetic biochemical processes determine  $^2\text{H}$ -fractionation during compound biosynthesis in plants does, however, not exist.

Here, we present new empirical data and a conceptual biochemical model that highlights how and where  $^2\text{H}$ -fractionation occurs during photosynthetic and post-photosynthetic processes in plants. The conceptual model is designed to mechanistically understand different magnitudes in  $^2\text{H}$ - $\epsilon_{\text{bio}}$  in different plant-derived organic compound classes and to link the variability of  $^2\text{H}$ - $\epsilon_{\text{bio}}$  within a given compound to metabolic processes in plants. As such, our model will provide new opportunities for the interpretation of  $\delta^2\text{H}$  values in plant-derived organic compounds and will in particular facilitate the use of  $\delta^2\text{H}$  values in plant-derived compounds to assess processes related to the carbon metabolism of plants.

We build our model on empirical H isotope data that we generated in two complementary experiments. In both experiments we tested the effects of the plants carbon metabolism on the hydrogen isotope composition of plant-derived carbohydrates and lipids by experimentally manipulating the photosynthetic carbohydrate supply to the plant. In the first experiment, we manipulated the photosynthetic carbohydrate supply to plants by limiting the  $\text{CO}_2$  that is available for the dark reaction of photosynthesis. Specifically, we grew six different vascular plant species under four different atmospheric  $\text{CO}_2$  concentrations ( $\text{pCO}_2$ ) stretching from estimated glacial maximum conditions (Tripathi *et al.*, 2009) and above the photosynthetic  $\text{CO}_2$  compensation point (Krenzer & Moss, 1969; Kestler *et al.*, 1975; Gerhart & Ward, 2010) to the averaged 2100 forecasts (Stocker *et al.*, 2013) (i.e. 150, 280, 400 and 800 ppm). In the second experiment, we manipulated the photosynthetic

carbohydrate supply to plants by limiting the light reaction of photosynthesis and forced the plants to meet their carbohydrate demands from reserves such as starch. For this purpose, we grew six different vascular plant species, which exhibit an autotrophic carbon metabolism when grown under natural environmental conditions, from bulbs, large seeds or tubers, that contain large carbohydrate reserves for 12 weeks under four different light treatments (0, 8, 115 and 355  $\mu\text{mol photons m}^{-2} \text{s}^{-1}$ ).

While all H atoms in plant-derived organic compounds originate from water, photosynthetic and post-photosynthetic H isotope fractionation in plants strongly depend on the biochemical origin of H atoms during biosynthesis (Fig. 1). Three biochemical origins of H in plants are important in this respect: (i) The organic precursor molecules in a biosynthetic pathway, e.g. the H atoms of ribulose-1,5-bisphosphate that are transferred to the 2 triose phosphates (TP) synthesized in the Calvin cycle or the acetyl-CoA hydrogens in the fatty acid biosynthetic pathway (Sachse et al., 2012). (ii) Redox cofactors, e.g. the biological reducing agent nicotinamide adenine dinucleotide phosphate (NADPH), that provide an important part of the H atoms in organic compounds (Kazuki et al., 1980). (iii) The cellular water, which is incorporated into organic molecules either by H addition to  $\text{sp}^2$  hybridized-C atoms (i.e.  $\text{C}=\text{C}$ ), for example by the fumarase reaction in the TCA cycle (Blanchard & Cleland, 1980), or by (partial) exchange of C-bound H atoms in  $\text{CH}_2$ -groups adjacent to CO-groups e.g. by the triosephosphate isomerase via an enolic structure in the glycolysis (Maister et al., 1976).

To identify for our model how changes in the plant's carbon metabolism affect the biochemical origin of H in photosynthetic and post-photosynthetic biochemical processes, we analysed in our experiments the  $\delta^2\text{H}$  values of two different compound classes that differ in their biochemical pathways and thus in the contribution of H from different biochemical origins in their biosynthesis. These compound classes are carbohydrates (i.e.  $\alpha$ -cellulose) and lipids (i.e. *n*-alkanes).

## Materials & methods

**CO<sub>2</sub> experiment:** In four climate controlled greenhouses, we grew six different C<sub>3</sub> plant species from seeds (i.e. two grasses: *Arrhenatherum elatius* and *Festuca rubra*; two legumes: *Trifolium pratense* and *Lathyrus pratensis*; two forbs: *Centaurea jacea* and *Plantago lanceolata*) under four atmospheric CO<sub>2</sub> concentrations (150, 280, 400 and 800 ppm). All the other parameters have been kept constant during the experiment (T = 20°C during day and 10°C during night, rH = 60%, LD 14:10 cycle). Plants were grown in 3 replicates. After 12 weeks, the plants were harvested and oven-dried at 50°C. Leaves were sampled at five different days during the growing experiments for leaf water extractions and conserved frozen in Exetainer vials (gas tight).

**Light experiment:** In four climate controlled growth chambers, four different light treatments (0, 8, 115 and 355  $\mu\text{mol photons m}^{-2} \text{s}^{-1}$ ) were constantly applied on six different plant species (i.e. C<sub>3</sub> species: *Solanum tuberosum*, *Ipomoea* sp., *Helianthus tuberosus*, *Zingiber officinale*, *Allium cepa*, and finally *Zea mays* subsp. *Mays*, a C<sub>4</sub> plant), while the other parameters were kept constant (T = 25°C, rH = 60%). Plants were grown in four replicates mostly from large storage organs (i.e. tubers for *Solanum tuberosum*, *Ipomoea* sp., and *Helianthus tuberosus*, roots for *Zingiber officinale*, bulb for *Allium cepa*, and seeds for *Zea mays* subsp. *mays*) in the dark and low light treatments. After 12 weeks of growing, the plants were harvested and oven-dried at 50°C. Leaves were sampled at 11 different days during the growing experiments for leaf water extractions and conserved frozen in Exetainer vials. The environmental variables for the light and the CO<sub>2</sub> experiments are summarized in the tables S3 and S4.

**Chemical purifications:** For all specimens, leaf wax *n*-alkanes and  $\alpha$ -cellulose were extracted and purified from the dried plant material. The lipids (including *n*-alkanes) were extracted in combusted glass vials from 1 g of dry leaves using 30 mL of a dichloromethane (DCM) : methanol mixture (9:1) under an ultrasonic bath during 15 min. Hydrocarbons (including *n*-alkanes) were subsequently isolated for isotope analysis from other lipids by column chromatography by eluting 10 mL hexane in 6 mL combusted glass silica-gel columns. The columns were pre-prepared by filling about three quarters (i.e. 2 g) of the column volume with silica-gel (0.040-0.063 mm, 99.5% pure). The columns were rinsed with 10 mL acetone, 10 mL DCM and 10 mL hexane and finally chemically activated in a desiccation oven at 60°C over-night. The

other lipids, including sterols and fatty acids, were eluted after the *n*-alkanes with a DCM : methanol mixture (9:1) and preserved for future analyses. For more details on the method see Peters *et al.* (2005).

For H isotope analyses on  $\alpha$ -cellulose, the cellulose was purified according to the method presented by Gaudinski *et al.* (2005). Briefly, about 150 mg of dry leaves was washed off from all lipids in Ankom bags by reflux in a Soxhlet apparatus with a toluene: ethanol (95%) mixture (2:1) for about 24 hrs under high heat, and then under ethanol only, until the solvent in the Soxhlet chamber was clear. Following this lipid removal, lignin was oxidised and washed away from the samples with a bleaching solution of sodium chloride and acetic acid (pH 4) under ultrasonic bath at 70°C for about 24 hrs. Finally, the  $\alpha$ -cellulose was purified from holocellulose with a 15% NaOH cold solution also under ultrasonic bath.

All plant-extractable leaf water was quantitatively extracted on a cryogenic water extraction line as described in West *et al.* (2006) and analyzed for its  $\delta^2\text{H}$  values (see tables S1 and S2). The frequent leaf water monitoring throughout both experiments allowed us to deduce an accurate  $^2\text{H}\text{-}\epsilon_{\text{bio}}$  for *n*-alkanes and  $\alpha$ -cellulose excluding the effect of leaf water evaporative  $^2\text{H}$ -enrichment as:

$$\text{Eq. 1. } ^2\text{H} - \epsilon_{\text{bio}} = (1000 \cdot (\text{organic compound } \delta^2\text{H} + 1000) / (\text{leaf water } \delta^2\text{H} + 1000) - 1)$$

Even though heterogeneity in leaf water  $\delta^2\text{H}$  exists (Cernusak *et al.*, 2016), we used the mean bulk leaf  $\delta^2\text{H}$  water to calculate  $^2\text{H}\text{-}\epsilon_{\text{bio}}$  since sub-cellular leaf water  $\delta^2\text{H}$  values cannot be measured and we did not want to add additional uncertainties into our empirical data by modelling them. We decided – as typically done in the literature – to calculate the  $^2\text{H}\text{-}\epsilon_{\text{bio}}$  as the difference between mean bulk foliar water (measured several times during the experiment) and the organic  $\delta^2\text{H}$  values (measured at the end of the experiment).

While homologous *n*-alkanes  $\delta^2\text{H}$  values can vary, even within a single plant (e.g. Chikaraishi & Naraoka, 2003; Magill *et al.*, 2013), we measured  $\delta^2\text{H}$  values of the C29 *n*-alkane as it was the only compound abundant enough for GC-IRMS measurements that occurred in all species. To allow the comparison of treatment effects on  $^2\text{H}\text{-}\epsilon_{\text{bio}}$



across all six species, we standardized the  $^2\text{H}\text{-}\epsilon_{\text{bio}}$  response of a species to its overall mean  $^2\text{H}\text{-}\epsilon_{\text{bio}}$  in both experiments (i.e.  $\Delta^2\text{H}\text{-}\epsilon_{\text{bio}}$ ).

**Isotope analyses:** The water  $\delta^2\text{H}$  values have been measured on a DeltaPlus XP isotope ratio mass spectrometer (IRMS) coupled to a high temperature conversion elemental analyzer (TC/EA) via a conFloIII (Gehre *et al.*, 2004). Following the method described by Sessions (2006),  $\delta^2\text{H}$  values on *n*-alkanes have been measured on a second Delta V plus stable isotope ratio mass spectrometer (IRMS) coupled to a Trace GC Ultra and a GC Isolink via a ConFlow IV. The cellulose  $\delta^2\text{H}$  values of the non-exchangeable H atoms were measured following an equilibration of the exchangeable H atoms as described by Schimmelmann (1991), Filot *et al.* (2006) and Sauer *et al.* (2009) using a TC/EA coupled to a Delta Advantage IRMS.

**Data analyses:** We fitted hyperbolic functions (expressing the balance between photosynthetic and post-photosynthetic effects on  $\Delta^2\text{H}\text{-}\epsilon_{\text{bio}}$ ) enhanced with linear functions (expressing the possible influence of photorespiration (Ehlers *et al.*, 2015)) into the relationships between the independent variables we manipulated in the two experiments and  $\Delta^2\text{H}\text{-}\epsilon_{\text{bio}}$ :  $\delta^2H = a + b/x + c \cdot d \cdot x/(c \cdot x + d)$ , where  $x$  is either the light intensity or the  $\text{pCO}_2$  values and  $a$  to  $d$  represent model-calculated parameters. At the positive end, the photosynthetic processes dominate and the inputs of new assimilates and light derived NADPH are at a maximum value and drive  $\Delta^2\text{H}\text{-}\epsilon_{\text{bio}}$  towards negative values. At the negative end, the pool of photosynthetic carbohydrate supply is low, due to little amount of, or no, new assimilates, resulting in an infinite cycling of individual compounds in this pool and driving toward positive values of  $\Delta^2\text{H}\text{-}\epsilon_{\text{bio}}$ .

## Results and discussion

Both, the  $\text{CO}_2$  and light limitation experiments revealed that  $^2\text{H}\text{-}\epsilon_{\text{bio}}$  varied systematically in different compound classes in response to the photosynthetic carbohydrate supply. This indicates that changes in plant C metabolism have strong effects on  $^2\text{H}$ -fractionation during the biosynthesis of organic compounds in plants (Figs. 2 and 3).

In the first experiment, we found strong effects of pCO<sub>2</sub> on leaf water evaporative <sup>2</sup>H-enrichment in all six CO<sub>2</sub> treated plants (Fig. 2a). The effects of pCO<sub>2</sub> on leaf water δ<sup>2</sup>H values can be explained by the CO<sub>2</sub> sensitivity of stomatal conductance and resulting effects on the evaporative <sup>2</sup>H-enrichment of leaf water. In the Péclet-modified Craig-Gordon model, transpiration has been shown to reduce <sup>2</sup>H-enrichment of leaf water due to the dilution of leaf water with unenriched source water (Cernusak et al., 2016). The increase in leaf water δ<sup>2</sup>H values at higher pCO<sub>2</sub> that we observed in our experiment can therefore be explained by reduced stomatal conductance and transpiration, resulting in a decreased Péclet effect. δ<sup>2</sup>H values differed strongly between α-cellulose and *n*-alkanes and showed no unidirectional relationship with pCO<sub>2</sub> (Fig. 2b, d). Importantly, when the effects of leaf water evaporative <sup>2</sup>H-enrichment on δ<sup>2</sup>H values of α-cellulose and *n*-alkanes were accounted for by subtracting leaf water δ<sup>2</sup>H values from δ<sup>2</sup>H values of organic compounds (and calculating as such <sup>2</sup>H-ε<sub>bio</sub> for a given compound class and species using Eq. 1), we observed that the <sup>2</sup>H-ε<sub>bio</sub> for α-cellulose and *n*-alkanes was strongly affected by pCO<sub>2</sub> in all six species (Fig. S1). When the inherent species specific variability in <sup>2</sup>H-ε<sub>bio</sub> was accounted for by standardizing the treatment response of <sup>2</sup>H-ε<sub>bio</sub> for a given compound around the overall mean <sup>2</sup>H-ε<sub>bio</sub> of a species (i.e. calculating Δ<sup>2</sup>H-ε<sub>bio</sub>), it became evident that the pCO<sub>2</sub> effects on <sup>2</sup>H-ε<sub>bio</sub> were consistent in trend and magnitude across all species and for both compound classes (Fig. 2c, e). Effects were strongest at the lowest pCO<sub>2</sub> level, where we assume that the plant's carbon metabolism became limited by photosynthetic carbohydrate supply (Drake et al., 1997). For both α-cellulose and *n*-alkanes, <sup>2</sup>H-ε<sub>bio</sub> at 150 ppm was 20‰ and 16‰ more positive (at probability p<0.05 and p<0.001, respectively, using F-values from two-way ANOVA) than at pre-industrial pCO<sub>2</sub> (i.e. 280 ppm). However, <sup>2</sup>H-ε<sub>bio</sub> did not become increasingly negative beyond 400 ppm pCO<sub>2</sub>.

In the second experiment, we found strong effects of the available photosynthetically active radiation (PhAR) on leaf water evaporative <sup>2</sup>H-enrichment in all six plant species (Fig. 3a). The effects of light intensity on leaf water δ<sup>2</sup>H values can be explained by the light sensitivity of stomatal conductance and resulting effects on the evaporative <sup>2</sup>H-enrichment of the leaf water (Cernusak et al., 2016). δ<sup>2</sup>H values differed strongly between α-cellulose and *n*-alkanes and δ<sup>2</sup>H values of both compounds showed a

negative relationship with increasing PhAR (Fig. 3b, d). When the effects of leaf water evaporative  $^2\text{H}$ -enrichment were accounted for by subtracting leaf water  $\delta^2\text{H}$  values from  $\delta^2\text{H}$  values of organic compounds, we found that  $\varepsilon_{\text{bio}}$  for  $\alpha$ -cellulose and  $n$ -alkanes was strongly affected by light intensity in all six species (Fig. S2). The effect was greatest under fully dark conditions, when plants were completely limited in their photosynthetic carbohydrate supply and were forced to meet 100% of their carbon and energy demands from carbohydrate reserves or other organic molecules (i.e. sugars, proteins, lipids). When  $^2\text{H}$ - $\varepsilon_{\text{bio}}$  responses were standardized (i.e.  $\Delta^2\text{H}$ - $\varepsilon_{\text{bio}}$ ) across species to allow comparison of the treatment effects across species, we detected that the treatment responses in  $\Delta^2\text{H}$ - $\varepsilon_{\text{bio}}$  were remarkably consistent in direction and magnitude across species but differed in magnitude between the two compound classes (Fig 3c, e). In full dark,  $\Delta^2\text{H}$ - $\varepsilon_{\text{bio}}$  for  $\alpha$ -cellulose and  $n$ -alkanes was more positive than  $\Delta^2\text{H}$ - $\varepsilon_{\text{bio}}$  of plants that grew under light (Fig. 3c, e). For  $\alpha$ -cellulose and  $n$ -alkanes,  $\Delta^2\text{H}$ - $\varepsilon_{\text{bio}}$  at 0 PhAR was 22‰ and 43‰ more positive ( $p < 0.05$  and  $p < 0.001$ , respectively) than at higher PhAR (i.e.  $354 \mu\text{mol m}^{-2} \text{s}^{-1}$ ). However,  $^2\text{H}$ - $\varepsilon_{\text{bio}}$  did not become increasingly negative beyond  $115 \mu\text{mol m}^{-2} \text{s}^{-1}$  in either compound class.

Yakir & DeNiro (1990) and later Luo & Sternberg (1992) have previously shown that cellulose  $\delta^2\text{H}$  values increase when a plant's carbon metabolism was forced into a state of low photosynthetic carbohydrate supply. We show here, that these effects are relevant not only for cellulose but also for other compound classes such as lipids but that the magnitude by which the plant's carbon metabolism affects  $^2\text{H}$ - $\varepsilon_{\text{bio}}$  differed for compound classes and was dependent on the treatment (Figs. 2 and 3). This indicates that different biochemical  $^2\text{H}$ -fractionation processes determine not only  $^2\text{H}$ - $\varepsilon_{\text{bio}}$  in different compound classes but that these different biochemical  $^2\text{H}$ -fractionation processes are differently affected by changes in the plant's carbon metabolism. This in turn provides us with the opportunity to establish - based on the known biochemical pathways - a conceptual biochemical model that identifies how and where H isotope fractionations occur during the biosynthesis of different plant compounds and to conceptualize how changes in a plant's carbon metabolism affect the  $^2\text{H}$ -fractionations for a given compound (Fig. 4).

**Photosynthetic  $^2\text{H}$ -fractionation:** Photosynthetic  $^2\text{H}$ -fractionation occurs in the chloroplast during the light reaction of photosynthesis where ferredoxin-NADP<sup>+</sup> reductase produces NADPH with reduced H that is strongly  $^2\text{H}$ -depleted compared to leaf water (Luo et al., 1991). This  $^2\text{H}$ -depleted H pool in NADPH is subsequently introduced into organic compounds in the Calvin cycle to form a glyceraldehyde-3-phosphate (GAP) that will be  $^2\text{H}$ -depleted compared to leaf water and form a major constituent of the triosephosphate (TP) pool (Fig. 4). To our knowledge, the only attempt to estimate the magnitude of photosynthetic  $^2\text{H}$ -fractionation was by Yakir & DeNiro (1990), who calculated a value of -171‰ for cellulose in the aquatic plant *Lemna gibba*. While our experiments were not designed to isolate the magnitude of the photosynthetic component of  $^2\text{H}$ - $\epsilon_{\text{bio}}$ , we found that variations in PhAR above 115  $\mu\text{mol m}^{-2} \text{s}^{-1}$  did not affect  $^2\text{H}$ - $\epsilon_{\text{bio}}$  of  $\alpha$ -cellulose and *n*-alkanes in any of the six species that we investigated. This is the case even though net photosynthetic rates increased with increasing light intensity in all species (Fig S3). We thus conclude that photosynthetic  $^2\text{H}$ -fractionation is, for the light spectrum tested, independent of the rate of photosynthesis within a species and possibly stable for any given species. This finding is important as it suggests that variations in  $^2\text{H}$ - $\epsilon_{\text{bio}}$  in response to plant metabolic changes observed in this study are mainly the result of variations in post-photosynthetic H isotope fractionations.

**Effects of post-photosynthetic  $^2\text{H}$ -fractionation on  $\delta^2\text{H}$  values of different compound classes:** Irrespective of the treatment, we found  $\alpha$ -cellulose in both experiments to be less  $^2\text{H}$ -depleted compared to leaf water than lipids (Figs. 2 and 3). This was for all species when these were grown at sufficient photosynthetic carbohydrate supply rates, i.e. at  $\text{pCO}_2 \geq 280$  ppm or a light intensity of  $\geq 8 \mu\text{mol photon m}^{-2} \text{s}^{-1}$ . This is consistent with previous studies that have reported similar patterns for cellulose or starch (Epstein *et al.*, 1976; Sternberg *et al.*, 1984a). Given the strong  $^2\text{H}$ -depletion during photosynthetic H isotopes fractionation processes (Yakir & DeNiro, 1990), these values suggest that post-photosynthetic  $^2\text{H}$ -fractionations have a strong effect on the observed  $\delta^2\text{H}$  values of carbohydrates in plants.

Post-photosynthetic  $^2\text{H}$ -enrichment commences in the TP pool that is in rapid reciprocal exchange with the hexosephosphate (HP) pool in a futile cycle from which

carbohydrates are synthesized (Buchanan et al., 2015) (Fig. 4). Several processes can lead to the post-photosynthetic  $^2\text{H}$ -enrichment of the TP and HP pools as outlined in our conceptual model (Fig. 1 and 4): (i) The synthesis of GAP in the Calvin cycle allows (partial) exchange of C-bound H atoms with the surrounding ( $^2\text{H}$ -enriched) cellular water in  $\text{CH}_2$ -groups adjacent to CO-groups via an enolic structure (Rieder & Rose, 1959; Maister *et al.*, 1976; Knowles & Albery, 1977), leading to an  $^2\text{H}$ -enrichment of the GAP pool. Wang *et al.* (2009) have calculated a theoretical equilibrium fractionation of organic H for H-C-OH positions up to 96‰, illustrating that C-bound H exchange with water can drive GAP and consequently carbohydrates towards positive  $\delta^2\text{H}$  values. (ii) In new photosynthetically derived GAP, only one out of four C-bound H atoms is derived from  $^2\text{H}$ -depleted NADPH from the light reaction of photosynthesis. The other C-bound H atoms are coming from the precursor molecule 3-phosphoglyceraldehyde (3-PGA) that is  $^2\text{H}$ -enriched compared to NADPH because of previous H exchanges with cellular water as described above. (iii) During the production of HP, where two trioses are bound to form fructose 1,6-bisphosphate, one out of four C-bound H atoms is lost to the surrounding water (Rose & Rieder, 1958; Hall *et al.*, 1999). As light isotopologues will react faster in this reaction, this process leads to a  $^2\text{H}$ -enrichment of the GAP pool (Schmidt et al., 2015). (iv) The enzyme phosphoglucose isomerase used to interconvert glucose 6-phosphate and fructose 6-phosphate might  $^2\text{H}$ -enrich the HP pool even further during that step by allowing partial exchange of specific H atoms (Fig. 1) with the surrounding cellular water (Schleucher et al., 1999).

As a consequence of the different post-photosynthetic  $^2\text{H}$ -fractionation processes that lead to a  $^2\text{H}$ -enrichment of the TP and the HP pool, carbohydrates typically do not deviate as strongly in their  $\delta^2\text{H}$  values from leaf water as we would expect from the primary  $^2\text{H}$ -depletion of the NADPH pool that is generated in the light reaction of photosynthesis. While the above-described mechanisms are relevant for all carbohydrates,  $\delta^2\text{H}$  values can vary among different carbohydrates. Previous studies have for example shown that starch is  $^2\text{H}$ -depleted compared to cellulose (Smith & Epstein, 1970; Luo & Sternberg, 1991) and compared to leaf soluble sugars (Schleucher et al., 1999). This has been attributed to a  $^2\text{H}$ -depletion at position C2 caused by the pronounced disequilibrium of phosphoglucose isomerase (Schleucher et al., 1999). Analogous  $^3\text{H}$ -depletion at the same position was found by Dorrer *et al.* (1966).

*n*-Alkanes and lipids in general had more negative  $^2\text{H}\text{-}\epsilon_{\text{bio}}$  than  $\alpha$ -cellulose in our and in previous studies (Smith & Epstein, 1970; White, 1989; Schmidt *et al.*, 2003). This is despite the fact that the precursor molecule in lipid biosynthesis, phosphoenolpyruvate (PEP) and eventually acetyl-CoA, are originating from the same  $^2\text{H}$ -enriched TP pools, as the precursor molecules of carbohydrates (Buchanan *et al.*, 2015). In addition, the metabolic conversion of GAP to organic acids (i.e. PEP, pyruvate and malate) and from organic acids to acetyl-CoA involves the loss of  $^2\text{H}$ -depleted H to nicotinamide adenine dinucleotide (NADH) and NADPH during glycolysis and loss of  $^2\text{H}$ -depleted hydrogen in form of NADH, flavin adenine dinucleotide ( $\text{FADH}_2$ ), and in some cases NADPH, that occurs in the tricarboxylic acid (TCA) cycle (Rambeck & Bassham, 1973; Møller & Rasmusson, 1998; Igamberdiev & Gardeström, 2003; White *et al.*, 2012). Also, during the conversion of organic acids to acetyl-CoA and in the TCA cycle exchange of C-bound H atoms with surrounding  $^2\text{H}$ -enriched water occurs (Rambeck & Bassham, 1973; Silverman, 2002; Allen *et al.*, 2015). Organic acids as the precursor molecules of lipids should thus be more  $^2\text{H}$ -enriched than molecules in the TP pool. This is, however, not reflected in lipids because  $^2\text{H}$ -depleted NADPH is a critical source of H in their biosynthesis. In carbohydrates, approximately 15% of C-bound H atoms originate from  $^2\text{H}$ -depleted NADPH that is produced during the light reaction of photosynthesis in the chloroplast and by the oxPPP in the cytosol (Fig. 1). In contrast, about half of the C-bound H atoms originate from  $^2\text{H}$ -depleted NADPH in the autotrophic fatty acid and *n*-alkane biosynthesis (Kazuki *et al.*, 1980; Baillif *et al.*, 2009) (Fig. 5). As such, lipids in general and *n*-alkanes in particular are strongly  $^2\text{H}$ -depleted compared to carbohydrates in autotrophically growing plants.

**Metabolic effects on post-photosynthetic  $^2\text{H}$ -fractionation:** Our experiments revealed that plants that were forced into a state of low photosynthetic carbohydrate supply, whether by light or by  $\text{CO}_2$  limitation, have  $^2\text{H}\text{-}\epsilon_{\text{bio}}$  values for  $\alpha$ -cellulose and *n*-alkanes that are significantly less negative than those of plants growing under higher photosynthetic carbohydrate supply. The general trend of this effect was consistent in the two experiments and suggests that the post-photosynthetic  $^2\text{H}$ -fractionation processes described in detail below lead to more positive  $\delta^2\text{H}$  values when plants operate in a state of low photosynthetic carbohydrate supply (Luo & Sternberg, 1992; Yakir, 1992).

We identified two important post-photosynthetic biochemical processes that are responsible for the general  $^2\text{H}$ -enrichment of plant metabolites under low photosynthetic carbohydrate supply (see Fig. 4).

(I) We assume that a substrate-limited Calvin cycle as induced by our two experiments results in smaller TP and HP pools and consequently a higher turnover of the individual molecules in a pool at a given metabolic rate. We suggest that higher turnover rates of individual molecules in the TP and HP pools lead to increasing  $^2\text{H}$ -enrichment because the likelihood of equilibrium exchange of C-bound H in the TP and HP molecules with  $^2\text{H}$ -enriched cellular water increases (Luo & Sternberg, 1992; Augusti *et al.*, 2006). Similar processes have been suggested for the exchange of O atoms during the biosynthesis of cellulose (Yakir & DeNiro, 1990; Hill *et al.*, 1995; Sternberg *et al.*, 2003; Barbour, 2007). While two out of six C-bound H atoms on a glucose-6-phosphate (i.e. C2 & C3) are always exchanged with the surrounding cellular water during the biosynthesis from ribulose-1,5-bisphosphate, the two C-bound H atoms on position C4 and C5 are only partially exchanged with the surrounding water (Rose & Rieder, 1958; Rieder & Rose, 1959; Fiedler *et al.*, 1967; Maister *et al.*, 1976; Knowles & Albery, 1977) (Fig. 1). A higher cycling rate of these molecules increases thus the chance for equilibration to happen on positions C4 and C5 with the surrounding  $^2\text{H}$ -enriched cellular water. This in turn will lead to a  $^2\text{H}$ -enrichment of the molecules in the TP and HP pool when photosynthetic carbohydrate supply is low.

(II) Sharkey & Weise (2015) postulate that at low photosynthetic carbohydrate supplies, the Calvin cycle is stabilized by means of the oxPPP replenishing the Calvin cycle intermediates with starch-derived pentose phosphates. Although starch is  $^2\text{H}$  depleted, the first enzyme of the oxPPP (glucose-6-phosphate dehydrogenase) has been shown to strongly  $^2\text{H}$ -enrich glucose-6-phosphate at C1 (Hermes *et al.*, 1982). This will lead to  $^2\text{H}$ -enrichment in glucose-6-phosphate and derivatives synthesized thereof when the oxPPP is upregulated (Wieloch *et al.* unpublished). Rearrangement of the photosynthetic carbohydrate metabolism in response to low photosynthetic carbohydrate supply might also induce a shift of stromal phosphoglucose isomerase towards equilibrium (Schleucher *et al.*, 1999). This would result in the biosynthesis of  $^2\text{H}$ -enriched transitory starch with downstream carbohydrates produced from the degradation of this starch also being  $^2\text{H}$ -enriched (Wieloch *et al.* unpublished).

In essence it is a combination of different biochemical processes that act in concert and lead to plant organic compounds becoming  $^2\text{H}$ -enriched when photosynthetic carbohydrate supply to a plant's metabolism is low.

Interestingly, metabolic effects on  $^2\text{H}$ - $\epsilon_{\text{bio}}$  values for  $\alpha$ -cellulose were identical in both experiments. In contrast, effects on  $^2\text{H}$ - $\epsilon_{\text{bio}}$  values for *n*-alkanes were much stronger when photosynthetic carbohydrate supply was reduced via the light reaction and plants were forced to utilize reserve carbohydrates as compared to photosynthetic carbohydrate supply being reduced via low  $\text{pCO}_2$  and a limitation of the dark reaction of photosynthesis (Figs. 2 and 3). These observations are in line with the conceptual biochemical model for metabolic effects on the hydrogen isotope composition of plant organic compounds that we outlined above and can thus be used to validate our above considerations. Under low  $\text{pCO}_2$  and under low light the biochemical source of H in the biosynthesis of carbohydrates is identical and comes from precursor molecules such as transitory or reserve starch that is converted to TP and HP that become  $^2\text{H}$ -enriched under low photosynthetic carbohydrate supply (Fig. 1, 4). In contrast, the main source of H in lipids comes directly from NADPH (Fig. 1, 5). As the supplies of NADPH and the hydrogen isotope composition of NADPH from the light reaction of photosynthesis should not have been affected by our low  $\text{pCO}_2$  treatment, the main H-source of lipids was consequently also unaffected by the  $\text{CO}_2$  treatments. This explains why effects of low photosynthetic carbohydrate supplies triggered by low  $\text{pCO}_2$  were comparatively small for  $^2\text{H}$ - $\epsilon_{\text{bio}}$  of *n*-alkanes (Fig. 3c, e). In contrast, the metabolic effects on  $^2\text{H}$ - $\epsilon_{\text{bio}}$  were stronger for *n*-alkanes when photosynthetic carbohydrate supplies were manipulated by low light and plants depended entirely on reserve metabolites for the biosynthesis of new organic compounds. The reason for this is that the biosynthesis of lipids from reserve carbohydrates via organic acids and acetyl-CoA requires additional NADPH-derived H (Figs. 4 and 5). In the absence of light this H cannot come from NADPH produced in the light reaction of photosynthesis but needs to be derived from NADPH that is generated heterotrophically, mainly in the oxPPP, and that has been shown to be  $^2\text{H}$ -enriched compared to autotrophically reduced NADPH (Sessions *et al.*, 1999; Zhang *et al.*, 2009; Schmidt *et al.*, 2015). This suggests that in addition to the  $^2\text{H}$ -enrichment of the biochemical precursor pools driven by the biochemical processes outlined above, the incorporation of additional and heterotrophically produced  $^2\text{H}$ -



enriched NADPH, leads to larger metabolic effects on  $^2\text{H}$ - $\epsilon_{\text{bio}}$  of lipids when photosynthetic carbohydrate supplies are limited by the light reaction of photosynthesis.

We found no effects of increasing  $\text{pCO}_2 \geq 280$  ppm on  $^2\text{H}$ - $\epsilon_{\text{bio}}$  in either compound class. We suggest that this is because the size of the carbohydrate pools and/or the turnover of the molecules in the pools was constant at  $\text{pCO}_2 \geq 280$  ppm in our experiment. It has been shown previously that the activity of RuBisCO is down-regulated with the accumulation of soluble carbohydrates in the chloroplast or cytosol (Webber et al., 1994). We thus suggest that at  $\text{pCO}_2 \geq 280$  ppm the carbohydrate pool size was not increasing enough in our experiment to significantly affect  $^2\text{H}$ - $\epsilon_{\text{bio}}$  of  $\alpha$ -cellulose or  $n$ -alkanes. Similarly, we did not observe strong effects on  $^2\text{H}$ - $\epsilon_{\text{bio}}$  above  $5 \mu\text{mol photons m}^{-2} \text{s}^{-1}$  for  $n$ -alkanes and above  $115 \mu\text{mol photons m}^{-2} \text{s}^{-1}$  for  $\alpha$ -cellulose. This indicates that plants were already carbon autonomous with respect to the supply of fresh carbohydrates from photosynthesis or that the main source of NADPH in the biosynthesis of the compounds was coming from the light reaction of photosynthesis above these light intensities rather than from the degradation of the reserves via the oxPPP.

**Effects of photorespiration:** It has recently been shown that photorespiration can  $^2\text{H}$ -deplete the C-3 position of the 3-PGA (i.e. triose) (Ehlers et al., 2015). Photorespiration occurs because RuBisCO can also catalyze the oxygenation of ribulose-1,5-bisphosphate (RubP), a reaction that increases with declining  $\text{CO}_2$  concentrations (Bainbridge et al., 1995). This isotope effect of photorespiration should thus lead to  $^2\text{H}$ - $\epsilon_{\text{bio}}$  becoming progressively more negative at lower  $\text{CO}_2$  concentrations, where rates of photorespiration increase. An effect of photorespiration on  $^2\text{H}$ - $\epsilon_{\text{bio}}$  of  $\alpha$ -cellulose and  $n$ -alkanes was, however, not detectable in our  $\text{CO}_2$  experiment. As indicated in our model, photorespiration seems to introduce  $^2\text{H}$ -depleted H at the C-3 position of 3-PGA due to the introduction of  $^2\text{H}$ -depleted H atoms via the reaction ferredoxin glutamine:oxoglutarate aminotransferase during the photorespiratory pathways (Peterhansel et al., 2010) (Fig. 4). This  $^2\text{H}$ -depleted C-3 position, which is transferred to other positions without H isotope exchange during glucose and  $n$ -alkane biosynthesis (Fig. 1 and 5), can affect up to 1 out of 7 and 9 out of 59 C-bound H atoms in a glucose

and in a C<sub>29</sub>-alkane molecule, respectively at high rates of photorespiration (Ehlers et al., 2015). It seems that these effects are too small to be detected in the  $\delta^2\text{H}$  values of organic compounds or that the H isotopic changes associated with the cycling of the TP and HP pool and with the source of NADPH mask those of the photorespiration for  $\alpha$ -cellulose and *n*-alkanes.

**Effects of gluconeogenesis:** Plants growing at low photosynthetic carbohydrate supply can utilize not only starch reserves as illustrated in our model but also lipid reserves to serve as C and energy source for the biosynthesis of compounds via gluconeogenesis. This is particularly relevant for plants growing from oil containing seeds. Luo & Sternberg (1992) have shown that plants growing from low photosynthetic supply from carbohydrate reserves (i.e. starch) have cellulose  $\delta^2\text{H}$  values that are lower than plants growing from lipids. In plants with low photosynthetic carbohydrate supply that utilize lipids as their C and energy source, an important part of the precursor molecules for the production of new carbohydrates and lipids is acetyl-CoA, which is produced as a degradation product of the lipid  $\beta$ -oxidation that occurs via gluconeogenesis (Fig. 4). This important metabolic pathway results in a  $^2\text{H}$ -enrichment of the acetyl-CoA pool by producing  $^2\text{H}$ -depleted FADH<sub>2</sub> and NADH. Moreover, the action of enoyl CoA hydratase allows the exchange of C-bound H atoms with the surrounding  $^2\text{H}$ -enriched foliar water. In the subsequent glyoxalate cycle, where two acetyl-CoA are used to produce succinate that will enter the TCA cycle and produce a new PEP, malate dehydrogenase will further  $^2\text{H}$ -enrich the pool of succinate by producing  $^2\text{H}$ -depleted NADH. As a result, carbohydrates produced by plants from lipid reserves are  $^2\text{H}$ -enriched compared to carbohydrates that are produced from carbohydrate reserves (Agrawal & Canvin, 1971).

**Post-photosynthetic  $^2\text{H}$ -fractionation in plants with different photosynthetic pathways:** Differences in  $\delta^2\text{H}$  values of organic compounds have also been observed among plants that differ in their photosynthetic pathways (e.g. C<sub>3</sub>, C<sub>4</sub> and Crassulacean Acid Metabolism (CAM)) (Sternberg *et al.*, 1984a; Chikaraishi *et al.*, 2004; Smith & Freeman, 2006; Feakins & Sessions, 2010a; Zhou *et al.*, 2011; Sachse *et al.*, 2012; Gamarra *et al.*, 2016). Specifically, carbohydrates and lipids in C<sub>4</sub> plants have generally been reported to be  $^2\text{H}$ -enriched compared to those produced in C<sub>3</sub> plants. As suggested

by (Zhou *et al.*, 2016), the different anatomies of C<sub>3</sub> and C<sub>4</sub> plants influence <sup>2</sup>H-ε<sub>bio</sub> via C-bound H exchanges with water of different anatomical compartments. For instance, intermediate compounds in C<sub>4</sub> plants exchange C-bound H with waters of the mesophyll cells that is <sup>2</sup>H-enriched compared to water in the bundle sheath cells, contributing to organic molecules that are <sup>2</sup>H-enriched compared to those produced by C<sub>3</sub> plants. This is in particular since the water in the mesophyll cells in C<sub>4</sub> plants should be <sup>2</sup>H-enriched compared to the bulk leaf water values of C<sub>3</sub> plants (Gamarra *et al.*, 2016). Interestingly, our experimental treatments in the second experiment (where we included a C<sub>4</sub> plant *Zea mays*) show similar effects on <sup>2</sup>H-ε<sub>bio</sub> of the C<sub>4</sub> plant than on the other investigated C<sub>3</sub> species (Fig S1). This suggests that metabolic effects of low photosynthetic carbohydrate supply on the <sup>2</sup>H-ε<sub>bio</sub> of plant organic compounds are valid for plants with different photosynthetic pathways and that the δ<sup>2</sup>H values of those plants equally record a low photosynthetic carbohydrate supply and/or a fast cycling of molecules in the TP and HP pools.

<sup>2</sup>H-enrichment of organic compounds from CAM plants compared to organic compounds from C<sub>3</sub> plants that have been reported in the literature also agree with our conceptual model (Ziegler *et al.*, 1976; Feakins & Sessions, 2010b; Sachse *et al.*, 2012). During the day, when CAM plants release CO<sub>2</sub> via NAD(P)-malic enzyme (ME) from the malic acid and perform photosynthesis by using this CO<sub>2</sub>, the resulting C<sub>3</sub> compounds are used to produce starch via the same biosynthetic pathway, i.e. the gluconeogenesis, that is used after lipid degradation in regular C<sub>3</sub> plants. This mechanism leads to an intense cycling of malic acid and pyruvate and consequently a <sup>2</sup>H-enrichment of the involved molecules that ultimately lead to the TP and organic acid pool in the cytosol (Fig. 4). Interestingly, Sternberg *et al.* (1984a) observed that the cellulose produced by CAM plants is <sup>2</sup>H-enriched compared to lipids produced by the same plants. This is in agreement with our model and supports the idea that the cycling of organic precursors pools (such as pyruvate and malic acid or hexose and triose) and the extraction of light H via the reduction of NAD(P)<sup>+</sup> is an important driver for the <sup>2</sup>H-ε<sub>bio</sub> of carbohydrates. This cycling seems to be a less important driver of the <sup>2</sup>H-ε<sub>bio</sub> in lipids biosynthesis as their main source of H comes from the NADPH produced in the chloroplast (Fig. 4).

**$^2\text{H}$  as a proxy for the C metabolism of plants:** The motivation of our study was to identify how and where  $^2\text{H}$ -fractionation occurs during photosynthetic and post-photosynthetic biosynthetic processes in plants. With this, we want to provide a mechanistic basis for understanding differences in  $^2\text{H}$ - $\epsilon_{\text{bio}}$  for different compound classes in plants and, most importantly, to set the mechanistic ground for the application of plant  $\delta^2\text{H}$  values as proxy for a plant's C metabolism. Our experiments show substantial differences in the  $\delta^2\text{H}$  values of carbohydrates and lipids that can largely be explained by the higher proportion of NADPH-derived and  $^2\text{H}$ -depleted H in lipids compared to carbohydrates. We show strong effects of low photosynthetic carbohydrate supply on the biosynthetic hydrogen isotope fractionation for both, carbohydrates and lipids. For carbohydrates, the metabolic effects on  $^2\text{H}$ - $\epsilon_{\text{bio}}$  were independent of the causes of low carbohydrate supply to the plant and were surprisingly robust across species and compound classes. For lipids, effects were stronger when plants were forced to utilize reserve carbohydrates in their metabolism and to generate NADPH for the biosynthesis of lipids via heterotrophic pathways.

Being able to interpret metabolic variability in the  $\delta^2\text{H}$  values of plant organic compounds that is beyond hydrological forcing will help to resolve previously explained variability in the  $\delta^2\text{H}$  values of plant organic compounds in sediment records or in tree rings when these are applied as a (paleo-)hydrological signals. Most importantly, however, understanding the metabolic effects that shape the  $\delta^2\text{H}$  values of plant organic compounds will open new opportunities to utilize plant  $\delta^2\text{H}$  values to address the carbon metabolism of plants and ecosystems. While we show here, that photosynthetic carbohydrate supply has a key effect on the  $\delta^2\text{H}$  values of plant organic compounds, previous studies have already employed  $\delta^2\text{H}$  values of *n*-alkanes or cellulose to indicate the carbon autonomy of plant tissues, plant organs or entire plants (Gamarra & Kahmen, 2015; Newberry *et al.*, 2015; Kimak *et al.*, 2015; Gebauer *et al.*, 2016). With our conceptual biochemical model, we can now explain why organic compounds in non-C autonomous tissue with low photosynthetic carbohydrate supplies become  $^2\text{H}$ -enriched. By comparing effects on carbohydrates and lipids, we can even differentiate if limitations of the light or dark reaction cause plant tissue to be carbon limited.

The model we present here will be particularly instrumental to interpret non-hydrological signals in  $\delta^2\text{H}$  values of plant organic compounds when these are analysed in combination with  $\delta^{18}\text{O}$  values. This is, because  $\delta^{18}\text{O}$  values are driven only by hydrological drivers (source water  $\delta^{18}\text{O}$  and leaf water  $\delta^{18}\text{O}$  (Roden et al., 2000; Kahmen et al., 2011) and the combined analysis of  $\delta^2\text{H}$  and  $\delta^{18}\text{O}$  values should thus allow to disentangle hydrological and metabolic effects, e.g. in tree ring or sediment records. Such an application of  $\delta^2\text{H}$  values in plant organic compounds could allow for the first time to assess long-term metabolic responses of plants and ecosystems to global environmental change and to address important feedbacks between the coupled climate carbon cycle. While a quantitative link between a plants carbon metabolism and variability in the  $\delta^2\text{H}$  values will have to be established in future studies, the experiments that we present here, and the conceptual biochemical model that resulted from these experiments, set the foundation for establishing plant  $\delta^2\text{H}$  values as a fundamentally important new metabolic proxy that will be relevant for a broad range of disciplines, including plant physiology, plant breeding, ecology, biogeochemistry, paleoecology and earth system sciences.

## Acknowledgement

M.A.C. and A.K. were both funded by the ERC starting grant COSIWAX (ERC-2011-StG Grant Agreement No. 279518) to A.K. We thank Rolf Siegwolf (PSI) and Adam Kimak (Bern) for their help with the cellulose extractions and measurements.

## References

- Agrawal PK, Canvin DT. 1971.** The pentose phosphate pathway in relation to fat synthesis in the developing castor oil seed. *Plant Physiology* **47**: 672–675.
- Allen DK, Bates PD, Tjellström H. 2015.** Tracking the metabolic pulse of plant lipid production with isotopic labeling and flux analyses: Past, present and future. *Progress in Lipid Research* **58**: 97–120.
- Augusti A, Betson TR, Schleucher J. 2006.** Hydrogen exchange during cellulose synthesis distinguishes climatic and biochemical isotope fractionations in tree rings.

- 654 *New Phytologist* **172**: 490–499.
- 655 **Baillif V, Robins RJ, Le Feunteun S, Lesot P, Billault I. 2009.** Investigation of  
 656 fatty acid elongation and desaturation steps in *Fusarium lateritium* by quantitative  
 657 two-dimensional deuterium NMR spectroscopy in chiral oriented media. *Journal of*  
 658 *Biological Chemistry* **284**: 10783–10792.
- 659 **Bainbridge G, Madgwick P, Parmar S, Mitchell R, Paul M, Pitts J, Keys AJ,**  
 660 **Parry MAJ. 1995.** Engineering Rubisco to change its catalytic properties. *Journal of*  
 661 *Experimental Botany* **46**: 1269–1276.
- 662 **Barbour MM. 2007.** Stable oxygen isotope composition of plant tissue: a review.  
 663 *Functional Plant Biology* **34**: 83–94.
- 664 **Blanchard JS, Cleland WW. 1980.** Use of isotope effects to deduce the chemical  
 665 mechanism of fumarase. *Biochemistry* **19**: 4506–4513.
- 666 **Buchanan BB, Gruissem W, Vickers K, Jones RL. 2015.** *Biochemistry and*  
 667 *molecular biology of plants*. New York: Wiley and sons.
- 668 **Burgoyne TW, Hayes JM. 1998.** Quantitative production of H<sub>2</sub> by pyrolysis of gas  
 669 chromatographic effluents. *Analytical Chemistry* **70**: 5136–5141.
- 670 **Cernusak LA, Barbour MM, Arndt SK, Cheesman AW, English NB, Feild TS,**  
 671 **Helliker BR, Holloway Phillips MM, Holtum JAM, Kahmen A, et al. 2016.** Stable  
 672 isotopes in leaf water of terrestrial plants. *Plant, Cell and Environment* **39**: 1087–  
 673 1102.
- 674 **Cheesbrough TM, Kolattukudy PE. 1984.** Alkane biosynthesis by decarbonylation  
 675 of aldehydes catalyzed by a particulate preparation from *Pisum sativum*. *Proceedings*  
 676 *of the National Academy of Sciences* **81**: 6613–6617.
- 677 **Chikaraishi Y, Naraoka H. 2003.** Compound-specific  $\delta D$ – $\delta^{13}C$  analyses of *n*-  
 678 alkanes extracted from terrestrial and aquatic plants. *Phytochemistry* **63**: 361–371.
- 679 **Chikaraishi Y, Naraoka H, Poulson SR. 2004.** C and hydrogen isotopic  
 680 fractionation during lipid biosynthesis in a higher plant (*Cryptomeria japonica*).  
 681 *Phytochemistry* **65**: 323–330.
- 682 **Dawson KS, Osburn MR, Sessions AL, Orphan VJ. 2015.** Metabolic associations  
 683 with archaea drive shifts in hydrogen isotope fractionation in sulfate-reducing  
 684 bacterial lipids in cocultures and methane seeps. *Geobiology* **13**: 462–477.
- 685 **Dawson TE, Mambelli S, Plamboeck AH, Templer PH, Tu KP. 2002.** Stable  
 686 isotopes in plant ecology. *Annual Review of Ecology and Systematics* **33**: 507–559.
- 687 **Dorrer HD, Fedtke C, Trebst A. 1966.** Intramolekulare Wasserstoffverschiebung in  
 688 der Hexosephosphatisomerase Reaktion bei der photosynthetischen Stärkebildung in  
 689 Chlorella. *Chlorella. Z. Naturforschg*: 557–562.
- 690 **Drake BG, Gonzalez-Meler MA, Long SP. 1997.** More efficient plants: a  
 691 consequence of rising atmospheric CO<sub>2</sub>. *Annual review of plant physiology and plant*

692 *molecular biology* **48**: 609–639.

693 **Ehlers I, Augusti A, Betson TR, Nilsson MB, Marshall JD, Schleucher J. 2015.**  
 694 Detecting long-term metabolic shifts using isotopomers: CO<sub>2</sub>-driven suppression of  
 695 photorespiration in C3 plants over the 20<sup>th</sup> century. *Proceedings of the National*  
 696 *Academy of Sciences*: 201504493–10.

697 **Epstein S, Yapp CJ, Hall JH. 1976.** The determination of the D/H ratio of non-  
 698 exchangeable hydrogen in cellulose extracted from aquatic and land plants. *Earth and*  
 699 *Planetary Science Letters* **30**: 241–251.

700 **Estep MF, Hoering TC. 1980.** Biogeochemistry of the stable hydrogen isotopes.  
 701 *Geochimica et Cosmochimica Acta* **44**: 1197–1206.

702 **Feakins SJ, Sessions AL. 2010a.** Controls on the D/H ratios of plant leaf waxes in an  
 703 arid ecosystem. *Geochimica et Cosmochimica Acta* **74**: 2128–2141.

704 **Feakins SJ, Sessions AL. 2010b.** Crassulacean acid metabolism influences D/H ratio  
 705 of leaf wax in succulent plants. *Organic Geochemistry* **41**: 1269–1276.

706 **Fiedler F, Müllhofer G, Trebst A, Rose IA. 1967.** Mechanism of Ribulose-  
 707 Diphosphate Carboxydismutase Reaction. *European Journal of Biochemistry* **1**: 395–  
 708 399.

709 **Filot MS, Leuenberger M, Pazdur A, Boettger T. 2006.** Rapid online equilibration  
 710 method to determine the D/H ratios of non-exchangeable hydrogen in cellulose. *Rapid*  
 711 *Communications in Mass Spectrometry* **20**: 3337–3344.

712 **Gamarra B, Kahmen A. 2015.** Concentrations and  $\delta^2\text{H}$  values of cuticular n-alkanes  
 713 vary significantly among plant organs, species and habitats in grasses from an alpine  
 714 and a temperate European grassland. *Oecologia* **178**: 981–998.

715 **Gamarra B, Sachse D, Kahmen A. 2016.** Effects of leaf water evaporative 2H-  
 716 enrichment and biosynthetic fractionation on leaf wax n-alkane  $\delta^2\text{H}$  values in C3 and  
 717 C4 grasses. *Plant, Cell and Environment* **11**: 2390 – 2403.

718 **Gaudinski JB, Dawson TE, Quideau S, Schuur EAG, Roden JS, Trumbore SE,**  
 719 **Sandquist DR, Oh S-W, Wasylishen RE. 2005.** Comparative analysis of cellulose  
 720 preparation techniques for use with <sup>13</sup>C, <sup>14</sup>C, and <sup>18</sup>O isotopic measurements.  
 721 *Analytical Chemistry* **77**: 7212–7224.

722 **Gebauer G, Preiss K, Gebauer AC. 2016.** Partial mycoheterotrophy is more  
 723 widespread among orchids than previously assumed. *New Phytologist* **211**: 11–15.

724 **Gehre M, Geilmann H, Richter J, Werner RA, Brand WA. 2004.** Continuous flow  
 725 <sup>2</sup>H/<sup>1</sup>H and <sup>18</sup>O/<sup>16</sup>O analysis of water samples with dual inlet precision. *Rapid*  
 726 *Communications in Mass Spectrometry* **18**: 2650–2660.

727 **Gerhart LM, Ward JK. 2010.** Plant responses to low [CO<sub>2</sub>] of the past. *New*  
 728 *Phytologist* **188**: 674–695.

729 **Hall DR, Leonard GA, Reed CD, Watt CI, Berry A, Hunter WN. 1999.** The

730 crystal structure of *Escherichia coli* class II fructose-1,6-bisphosphate aldolase in  
 731 complex with phosphoglycolohydroxamate reveals details of mechanism and  
 732 specificity. *Journal of Molecular Biology* **287**: 383–394.

733 **Heldt HW, Piechulla B, Heldt F. 2005.** *Plant Biochemistry*. Elsevier.

734 **Hermes JD, Roeske CA, O'Leary MH, Cleland WW. 1982.** Use of multiple isotope  
 735 effects to determine enzyme mechanisms and intrinsic isotope effects - malic enzyme  
 736 and glucose-6-phosphate-dehydrogenase. *Biochemistry* **21**: 5106–5114.

737 **Hill SA, Waterhouse JS, Field EM, Switsur VR, Rees TA. 1995.** Rapid recycling  
 738 of triose phosphates in oak stem tissue. *Plant, Cell and Environment* **18**: 931–936.

739 **Hou J, D'Andrea WJ, Huang Y. 2008.** Can sedimentary leaf waxes record D/H  
 740 ratios of continental precipitation? Field, model, and experimental assessments.  
 741 *Geochimica et Cosmochimica Acta* **72**: 3503–3517.

742 **Igamberdiev AU, Gardeström P. 2003.** Regulation of NAD- and NADP-dependent  
 743 isocitrate dehydrogenases by reduction levels of pyridine nucleotides in mitochondria  
 744 and cytosol of pea leaves. *Biochimica et Biophysica Acta (BBA) - Bioenergetics* **1606**:  
 745 117–125.

746 **Kahmen A, Hoffmann B, Schefuß E, Arndt SK, Cernusak LA, West JB, Sachse  
 747 D. 2013a.** Leaf water deuterium enrichment shapes leaf wax n-alkane  $\delta D$  values of  
 748 angiosperm plants II: Observational evidence and global implications. *Geochimica et  
 749 Cosmochimica Acta* **111**: 50–63.

750 **Kahmen A, Sachse D, Arndt SK, Tu KP, Farrington H, Vitousek PM, Dawson  
 751 TE. 2011.** Cellulose  $\delta^{18}O$  is an index of leaf-to-air vapor pressure difference (VPD) in  
 752 tropical plants. *Proceedings of the National Academy of Sciences of the United States  
 753 of America* **108**: 1981–1986.

754 **Kahmen A, Schefuß E, Sachse D. 2013b.** Leaf water deuterium enrichment shapes  
 755 leaf wax n-alkane  $\delta D$  values of angiosperm plants I: Experimental evidence and  
 756 mechanistic insights. *Geochimica et Cosmochimica Acta* **111**: 39–49.

757 **Kazuki S, Akihiko K, Shigenobu O, Yousuke S, Tamio Y. 1980.** Incorporation of  
 758 hydrogen atoms from deuterated water and stereospecifically deuterium-labeled  
 759 nicotinamide nucleotides into fatty acids with the *Escherichia coli* fatty acid  
 760 synthetase system. *Biochimica et Biophysica Acta (BBA) - Lipids and Lipid  
 761 Metabolism* **618**: 202–213.

762 **Kestler DP, Mayne BC, Ray TB, Goldstein LD. 1975.** Biochemical components of  
 763 the photosynthetic CO<sub>2</sub> compensation point of higher plants. *Biochemical and  
 764 biophysical research communications* **66**: 1439–1446.

765 **Kimak A, Kern Z, Leuenberger M. 2015.** Qualitative distinction of autotrophic and  
 766 heterotrophic processes at the leaf level by means of triple stable isotope (C–O–H)  
 767 patterns. *Frontiers in Plant Science* **6**: 490.

768 **Knowles JR, Albery WJ. 1977.** Perfection in enzyme catalysis: the energetics of  
 769 triosephosphate isomerase. *Accounts of Chemical Research* **10**: 105–111.



- 770 **Krenzer EG, Moss DN. 1969.** C Dioxide Compensation in Grasses. *Crop Science* **9**:  
771 619–621.
- 772 **Liu Z, Huang Y. 2008.** Hydrogen isotopic compositions of plant leaf lipids are  
773 unaffected by a twofold pCO<sub>2</sub> change in growth chambers. *Organic Geochemistry*  
774 **39**: 478–482.
- 775 **Luo Y-H, Sternberg LDSLO. 1991.** Deuterium heterogeneity in starch and cellulose  
776 nitrate of cam and C<sub>3</sub> plants. *Phytochemistry* **30**: 1095–1098.
- 777 **Luo Y-H, Sternberg LDSLO. 1992.** Hydrogen and oxygen isotopic fractionation  
778 during heterotrophic cellulose synthesis. *Journal of Experimental Botany* **43**: 47–50.
- 779 **Luo Y-H, Sternberg LDSLO, Suda S, Kumazawa S, Mitsui A. 1991.** Extremely  
780 low D/H ratios of photoproduced hydrogen by cyanobacteria. *Plant and cell*  
781 *physiology* **32**: 897–900.
- 782 **Magill CR, Ashley GM, Freeman KH. 2013.** Water, plants, and early human  
783 habitats in eastern Africa. *Proceedings of the National Academy of Sciences of the*  
784 *United States of America* **110**: 1175–1180.
- 785 **Maister SG, Pett CP, Albery WJ, Knowles JR. 1976.** Energetics of triosephosphate  
786 isomerase: the appearance of solvent tritium in substrate dihydroxyacetone phosphate  
787 and in product. *Biochemistry* **15**: 5607–5612.
- 788 **Møller IM, Rasmusson AG. 1998.** The role of NADP in the mitochondrial matrix.  
789 *Trends in Plant Science* **3**: 21–27.
- 790 **Newberry SL, Kahmen A, Dennis P, Grant A. 2015.** *n*-Alkane biosynthetic  
791 hydrogen isotope fractionation is not constant throughout the growing season in the  
792 riparian tree *Salix viminalis*. *Geochimica et Cosmochimica Acta* **165**: 75–85.
- 793 **Pedentchouk N, Sumner W, Tipple B, Pagani M. 2008.**  $\delta^{13}\text{C}$  and  $\delta\text{D}$  compositions  
794 of *n*-alkanes from modern angiosperms and conifers: An experimental set up in  
795 central Washington State, USA. *Organic Geochemistry* **39**: 1066–1071.
- 796 **Peterhansel C, Horst I, Niessen M, Blume C, Kebeish R, Kürkcüoglu S,**  
797 **Kreuzaler F. 2010.** Photorespiration. *The Arabidopsis Book* **8**: e0130.
- 798 **Peters KE, Walters CC, Moldowan JM. 2005.** *The Biomarker Guide: Biomarkers*  
799 *and isotopes in the environment and human history*. Cambridge University Press.
- 800 **Rach O, Brauer A, Wilkes H, Sachse D. 2014.** Delayed hydrological response to  
801 Greenland cooling at the onset of the Younger Dryas in western Europe. *Nature*  
802 *Geoscience* **7**: 1–4.
- 803 **Rambeck WA, Bassham JA. 1973.** Tritium incorporation and retention in  
804 photosynthesizing algae. *Biochimica et Biophysica Acta (BBA) - General Subjects*  
805 **304**: 725–735.
- 806 **Rieder SV, Rose IA. 1959.** The mechanism of the triosephosphate isomerase  
807 reaction. *Journal of Biological Chemistry* **234**: 1007–1010.

808 **Roden JS, Lin G, Ehleringer JR. 2000.** A mechanistic model for interpretation of  
809 hydrogen and oxygen isotope ratios in tree-ring cellulose. *Geochimica et*  
810 *Cosmochimica Acta* **64**: 21–35.

811 **Rose IA, Rieder SV. 1958.** Studies on the mechanism on the aldolase reaction;  
812 isotope exchange reactions of muscle and yeast aldolase. *Journal of Biological*  
813 *Chemistry* **231**: 315–329.

814 **Sachse D, Billault I, Bowen GJ, Chikaraishi Y, Dawson TE, Feakins SJ, Freeman**  
815 **KH, Magill CR, McInerney FA, van der Meer MTJ, et al. 2012.** Molecular  
816 paleohydrology: Interpreting the hydrogen-isotopic composition of lipid biomarkers  
817 from photosynthesizing organisms. *Annual Review of Earth and Planetary Sciences*  
818 **40**: 221–249.

819 **Sachse D, Radke J, Gleixner G. 2004.** Hydrogen isotope ratios of recent lacustrine  
820 sedimentary n-alkanes record modern climate variability. *Geochimica et*  
821 *Cosmochimica Acta* **68**: 4877–4889.

822 **Sachse D, Radke J, Gleixner G. 2006.**  $\delta D$  values of individual *n*-alkanes from  
823 terrestrial plants along a climatic gradient – Implications for the sedimentary  
824 biomarker record. *Organic Geochemistry* **37**: 469–483.

825 **Sauer PE, Schimmelmann A, Sessions AL, Topalov K. 2009.** Simplified batch  
826 equilibration for D/H determination of non-exchangeable hydrogen in solid organic  
827 material. *Rapid Communications in Mass Spectrometry* **23**: 949–956.

828 **Schimmelmann A. 1991.** Determination of the Concentration and Stable Isotopic  
829 Composition of Nonexchangeable Hydrogen in Organic-Matter. *Analytical Chemistry*  
830 **63**: 2456–2459.

831 **Schirmer A, Rude MA, Li X, Popova E, del Cardayre SB. 2010.** Microbial  
832 biosynthesis of alkanes. *Science* **329**: 559–562.

833 **Schleucher J, Vanderveer P, Markley JL, Sharkey TD. 1999.** Intramolecular  
834 deuterium distributions reveal disequilibrium of chloroplast phosphoglucose  
835 isomerase. *Plant, Cell and Environment* **22**: 525–533.

836 **Schmidt H-L, Robins RJ, Werner RA. 2015.** Multi-factorial *in vivo* stable isotope  
837 fractionation: causes, correlations, consequences and applications. *Isotopes in*  
838 *environmental and health studies* **51**: 155–199.

839 **Schmidt H-L, Werner RA, Eisenreich W. 2003.** Systematics of  $^2H$  patterns in  
840 natural compounds and its importance for the elucidation of biosynthetic pathways.  
841 *Phytochemistry Reviews* **2**: 61–85.

842 **Sessions AL. 2006.** Isotope-ratio detection for gas chromatography. *Journal of*  
843 *Separation Science* **29**: 1946–1961.

844 **Sessions AL, Burgoyne TW, Schimmelmann A, Hayes JM. 1999.** Fractionation of  
845 hydrogen isotopes in lipid biosynthesis. *Organic Geochemistry* **30**: 1193–1200.

846 **Sharkey TD, Weise SE. 2016.** The glucose 6-phosphate shunt around the Calvin–

- 847 Benson cycle. *Journal of Experimental Botany* **67**: 4067–4077.
- 848 **Silverman RB. 2002.** *The organic chemistry of enzyme-catalyzed reactions*. San  
849 Diego : Academic Press.
- 850 **Smith BN, Epstein S. 1970.** Biogeochemistry of the stable isotopes of hydrogen and  
851 C in salt marsh biota. *Plant Physiology* **46**: 738–742.
- 852 **Smith FA, Freeman KH. 2006.** Influence of physiology and climate on  $\delta D$  of leaf  
853 wax *n*-alkanes from  $C_3$  and  $C_4$  grasses. *Geochimica et Cosmochimica Acta* **70**: 1172–  
854 1187.
- 855 **Sternberg LDSL, Anderson WT, Morrison K. 2003.** Separating soil and leaf water  
856  $^{18}O$  isotopic signals in plant stem cellulose. *Geochimica et Cosmochimica Acta* **67**:  
857 2561–2566.
- 858 **Sternberg LDSLO, DeNiro MJ, Ajie H. 1984a.** Stable hydrogen isotope ratios of  
859 saponifiable lipids and cellulose nitrate from CAM,  $C_3$  and  $C_4$  plants. *Phytochemistry*  
860 **23**: 2475–2477.
- 861 **Sternberg LDSLO, DeNiro MJ, Ting IP. 1984b.** C, hydrogen, and oxygen isotope  
862 ratios of cellulose from plants having intermediary photosynthetic modes. *Plant*  
863 *Physiology* **74**: 104–107.
- 864 **Stocker TF, Dahe Q, Plattner G-K. 2013.** Climate Change 2013: The Physical  
865 Science Basis. *Working Group I Contribution to the Fifth Assessment Report of the*  
866 *Intergovernmental Panel on Climate Change. Summary for Policymakers (IPCC,*  
867 *2013).*
- 868 **Tripati AK, Roberts CD, Eagle RA. 2009.** Coupling of  $CO_2$  and ice sheet stability  
869 over major climate transitions of the last 20 Million years. *Science* **326**: 1394–1397.
- 870 **Voet D, Voet JG. 2011.** *Biochemistry, 4th Edition*. New York: John Wiley & Sons.
- 871 **Wang Y, Sessions AL, Nielsen RJ, Goddard WA III. 2009.** Equilibrium  $2 H/1 H$   
872 fractionations in organic molecules. II: Linear alkanes, alkenes, ketones, carboxylic  
873 acids, esters, alcohols and ethers. ... *et Cosmochimica Acta* **73**: 7076–7086.
- 874 **Webber AN, Nie G-Y, Long SP. 1994.** Acclimation of photosynthetic proteins to  
875 rising atmospheric  $CO_2$ . *Photosynthesis Research* **39**: 413–425.
- 876 **West AG, Patrickson SJ, Ehleringer JR. 2006.** Water extraction times for plant and  
877 soil materials used in stable isotope analysis. *Rapid Communications in Mass*  
878 *Spectrometry* **20**: 1317–1321.
- 879 **White D, Drummond JT, Fuqua C. 2012.** *The Physiology and Biochemistry of*  
880 *Prokaryotes*. Oxford University Press, USA.
- 881 **White JWC. 1989.** Stable Hydrogen Isotope Ratios in Plants: A Review of Current  
882 Theory and Some Potential Applications. *Ecological Studies. Stable isotopes in*  
883 *ecological research*. New York, NY: Springer New York, 142–162.

884 **Wieloch T, Yu J, Ehlers I, Grabner M, Marshall JD, Schleucher J.** Metabolic  
885 regulation can be a major determinant of plant glucose D variability (*in preparation*).

886 **Yakir D. 1992.** Variations in the natural abundance of oxygen-18 and deuterium in  
887 plant carbohydrates. *Plant, Cell and Environment* **15**: 1005–1020.

888 **Yakir D, DeNiro MJ. 1990.** Oxygen and hydrogen isotope fractionation during  
889 cellulose metabolism in *Lemna gibba* L. *Plant Physiology* **93**: 325–332.

890 **Zhang X, Gillespie AL, Sessions AL. 2009.** Large D/H variations in bacterial lipids  
891 reflect central metabolic pathways. *Proceedings of the National Academy of Sciences*  
892 **106**: 12580–12586.

893 **Zhou Y, Grice K, Chikaraishi Y, Stuart-Williams H, Farquhar GD, Ohkouchi N.**  
894 **2011.** Phytochemistry. *Phytochemistry* **72**: 207–213.

895 **Zhou Y, Grice K, Stuart-Williams H, Hocart CH, Gessler A, Farquhar GD.**  
896 **2016.** Hydrogen isotopic differences between C3 and C4 land plant lipids:  
897 consequences of compartmentation in C4 photosynthetic chemistry and C3  
898 photorespiration. *Plant, Cell and Environment*.

899 **Ziegler H. 1989.** Hydrogen Isotope fractionation in plant tissues. Ecological Studies.  
900 Stable isotopes in ecological research. New York, NY: Springer New York, 105–123.

901 **Ziegler H, Osmond CB, Stichler W, Trimborn P. 1976.** Hydrogen isotope  
902 discrimination in higher-plants - Correlations with photosynthetic pathway and  
903 environment. *Planta* **128**: 85–92.

904

## 905    **Figures**

906    **Fig. 1.** Different biochemical origins of H atoms in the biosynthesis of plant organic compounds. We  
 907    illustrate the different origins for the biosynthesis of glucose but similar processes occur in all  
 908    biochemical pathways. Black H are coming from the precursor ribulose-1,5-bisphosphate, blue H are  
 909    coming from the surrounding water, green H are originating from NADPH. \* means that half of H atoms  
 910    at this position are coming from the cellular water, the rest are from the precursor molecule. Waves  
 911    represent H atoms that partially exchange with surrounding water through H addition to  $sp^2$  hybridized-  
 912    C atoms (i.e. C=C) or by (partial) exchange of C-bound H atoms in  $CH_2$ -groups adjacent to CO-groups.  
 913    Key enzymes and molecules are indicated by their following abbreviations: 3-PGA, 3-phosphoglycerate;  
 914    ALD, aldolase; DHAP, dihydroxyacetone phosphate; FBPase, fructose 1,6-bisphosphatase; FBP,  
 915    fructose 1,6-bisphosphate; F6P, fructose 6-phosphate; GAP, glyceraldehyde 3-phosphate; GAPDH,  
 916    glyceraldehyde 3-phosphate dehydrogenase;  $NADP^+$ , nicotinamide adenine dinucleotide phosphate;  
 917    PGI, phosphoglucose isomerase; PGK, phosphoglycerate kinase; PRP, photorespiratory pathway;  
 918    RuBisCO, ribulose-1,5-bisphosphate carboxylase/oxygenase; TPI, triosephosphate isomerase. The red  
 919    H represent the  $^2H$ -depleted atoms that can come from the 3-phosphoglycerate produced upon the  
 920    photosynthetic C oxidation during photorespiration (Rieder & Rose, 1959; Knowles & Albery, 1977;  
 921    Schleucher *et al.*, 1999; Augusti *et al.*, 2006; Buchanan *et al.*, 2015).

922    **Fig. 2.** Leaf water,  $\alpha$ -cellulose,  $n$ -alkane  $\delta^2H$  values and  $\Delta^2H-\epsilon_{bio}$  for  $\alpha$ -cellulose and  $n$ -alkanes under  
 923    different  $pCO_2$  averaged across all six species. The magnitude of  $^2H-\epsilon_{bio}$  can differ largely across different  
 924    species. To allow the comparison of treatment effects on  $^2H-\epsilon_{bio}$  across all six species we standardized  
 925    the  $^2H-\epsilon_{bio}$  response of a species to the  $pCO_2$  treatment around its overall mean  $^2H-\epsilon_{bio}$  in the experiment  
 926    (i.e.  $\Delta^2H-\epsilon_{bio}$ ). Each point corresponds to the averaged values 6 different species ( $n=6$ ) grown in 3  
 927    replicates from seeds under the different  $pCO_2$ . The  $^2H-\epsilon_{bio}$  curves for individual species are available of  
 928    Fig. S1.

930    **Fig. 3.** Leaf water,  $\alpha$ -cellulose,  $n$ -alkane  $\delta^2H$  values and the corresponding relative  $^2H-\epsilon_{bio}$  for  $\alpha$ -cellulose  
 931    and  $n$ -alkanes under different light intensities (photosynthetic active radiation, PhAR) averaged across  
 932    all six species. The magnitude of  $^2H-\epsilon_{bio}$  can differ largely across different species. To allow the  
 933    comparison of treatment effects on  $^2H-\epsilon_{bio}$  across all six species we standardized the  $^2H-\epsilon_{bio}$  response of  
 934    a species to the light treatment around its overall mean  $^2H-\epsilon_{bio}$  in the experiment (i.e.  $\Delta^2H-\epsilon_{bio}$ ). Each  
 935    point corresponds to the averaged values 6 different species ( $n=6$ ) grown in 3 replicates from the tuber  
 936    or roots under the different light intensity. The  $^2H-\epsilon_{bio}$  curves for individual species are available of Fig.  
 937    S2.

939    **Fig. 4.** Schematic view of H flow during processes leading to  $n$ -alkanes and  $\alpha$ -cellulose  $^2H-\epsilon_{bio}$ . The key  
 940    enzymes and pathways responsible for H flow are indicated by their following abbreviations and are  
 941    based on known biochemical pathways (Rose & Rieder, 1958; Rieder & Rose, 1959; Knowles & Albery,  
 942    1977; Cheesbrough & Kolattukudy, 1984; Schleucher *et al.*, 1999; Heldt *et al.*, 2005; Augusti *et al.*, 2006;  
 943    Zhang *et al.*, 2009; Schirmer *et al.*, 2010; Voet & Voet, 2011; Buchanan *et al.*, 2015; Ehlers *et al.*, 2015).  
 944    The Roman numerals indicate the two main post-photosynthetic biochemical processes that we suggest  
 945    to be responsible for the general  $^2H$ -enrichment of plant metabolites under low photosynthetic  
 946    carbohydrate supply: 2-OGDH, 2-oxoglutarate dehydrogenase; 6PGD, 6-phosphogluconate  
 947    dehydrogenase; ACP, acyl-carrier-protein; ALD, aldolase; ENO, enolase; Fd-GOGAT, ferredoxin  
 948    glutamine:oxoglutarate aminotransferase; FNR, ferredoxin- $NADP^+$  reductase; G6PDH, glucose-6-  
 949    phosphate dehydrogenase; GAP, glyceraldehyde 3-phosphate; GAPDH, glyceraldehyde 3-phosphate  
 950    dehydrogenase; IDH, isocitrate dehydrogenase; KA, ketoacyl; ME, malic enzyme; NADP, nicotinamide  
 951    adenine dinucleotide; NADPH, nicotinamide adenine dinucleotide phosphate; ME, malate  
 952    dehydrogenase; PDH, pyruvate dehydrogenase; PEP, phosphoenolpyruvate; PGI, phosphoglucose  
 953    isomerase; PK, pyruvate kinase; oxPPP, oxidative pentose phosphate pathway; TPI, triosephosphate  
 954    isomerase; TE, *trans*-enoyl; TPT, triose phosphate translocator; R, reductase; RuBisCO, ribulose-1,5-  
 955    bisphosphate carboxylase/oxygenase. Succinate dehydrogenase also produced  $FADH_2$  in the TCA cycle,  
 956    but is not represented on the scheme.

958    **Fig. 5.** Simplified view of the biochemical origins of H atoms in  $n$ -alkane biosynthesis. Black H represent  
 959    H atoms from the precursor acetyl-CoA. Green H originate from NADPH reduced by the light reaction  
 960    of photosynthesis in the chloroplast and or by oxPPP and other reactions in the endoplasmic reticulum.  
 961    Blue H are from H atoms in equilibrium with surrounding water. The fatty acids are generally elongated  
 962

963 until 16 or 18 Cs long in the chloroplast and until 32 Cs long in the endoplasmic reticulum; this might  
964 also imply different H sourcing (Cheesbrough & Kolattukudy, 1984; Zhang et al., 2009; Schirmer et al.,  
965 2010; Buchanan et al., 2015). The red H represent the  $^2\text{H}$ -depleted atoms that can come from the 3-  
966 phosphoglycerate produced upon the photosynthetic C oxidation. In a C<sub>29</sub>-alkane, of 60 H atoms, 28  
967 comes from NADPH, 14 from water, 17 from manolyl-ACP (which ultimately derives from acetyl-CoA  
968 and pyruvate).  
969

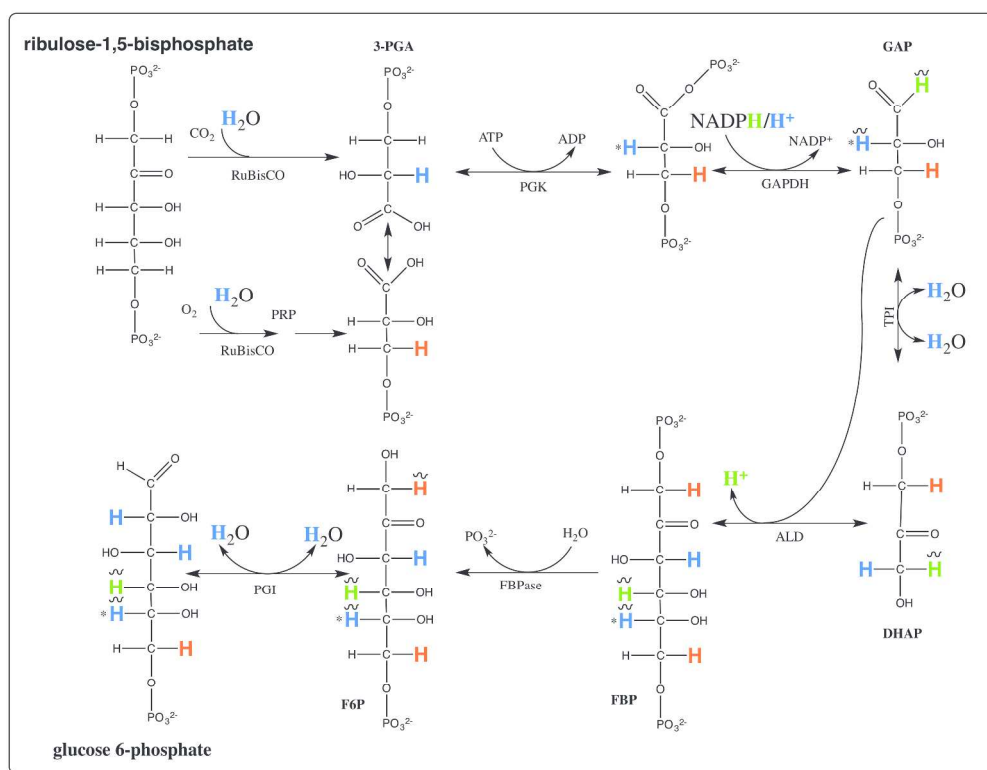


Fig. 1. Different biochemical origins of H atoms in the biosynthesis of plant organic compounds. We illustrate the different origins for the biosynthesis of glucose but similar processes occur in all biochemical pathways. Black H are coming from the precursor ribulose-1,5-bisphosphate, blue H are coming from the surrounding water, green H are originating from NADPH. \* means that half of H atoms at this position are coming from the cellular water, the rest are from the precursor molecule. Waves represent H atoms that partially exchange with surrounding water through H addition to sp<sup>2</sup> hybridized-C atoms (i.e. C=C) or by (partial) exchange of C-bound H atoms in CH<sub>2</sub>-groups adjacent to CO-groups. Key enzymes and molecules are indicated by their following abbreviations: 3-PGA, 3-phosphoglycerate; ALD, aldolase; DHAP, dihydroxyacetone phosphate; FBPase, fructose 1,6-bisphosphatase; FBP, fructose 1,6-bisphosphate; F6P, fructose 6-phosphate; GAP, glyceraldehyde 3-phosphate; GAPDH, glyceraldehyde 3-phosphate dehydrogenase; NADP<sup>+</sup>, nicotinamide adenine dinucleotide phosphate; PGI, phosphoglucose isomerase; PGK, phosphoglycerate kinase; PRP, photorespiratory pathway; RuBisCO, ribulose-1,5-bisphosphate carboxylase/oxygenase; TPI, triosephosphate isomerase. The red H represent the <sup>2</sup>H-depleted atoms that can come from the 3-phosphoglycerate produced upon the photosynthetic C oxidation during photorespiration (Rieder & Rose, 1959; Knowles & Alberty, 1977; Schleucher et al., 1999; Augusti et al., 2006; Buchanan et al., 2015)

305x235mm (300 x 300 DPI)

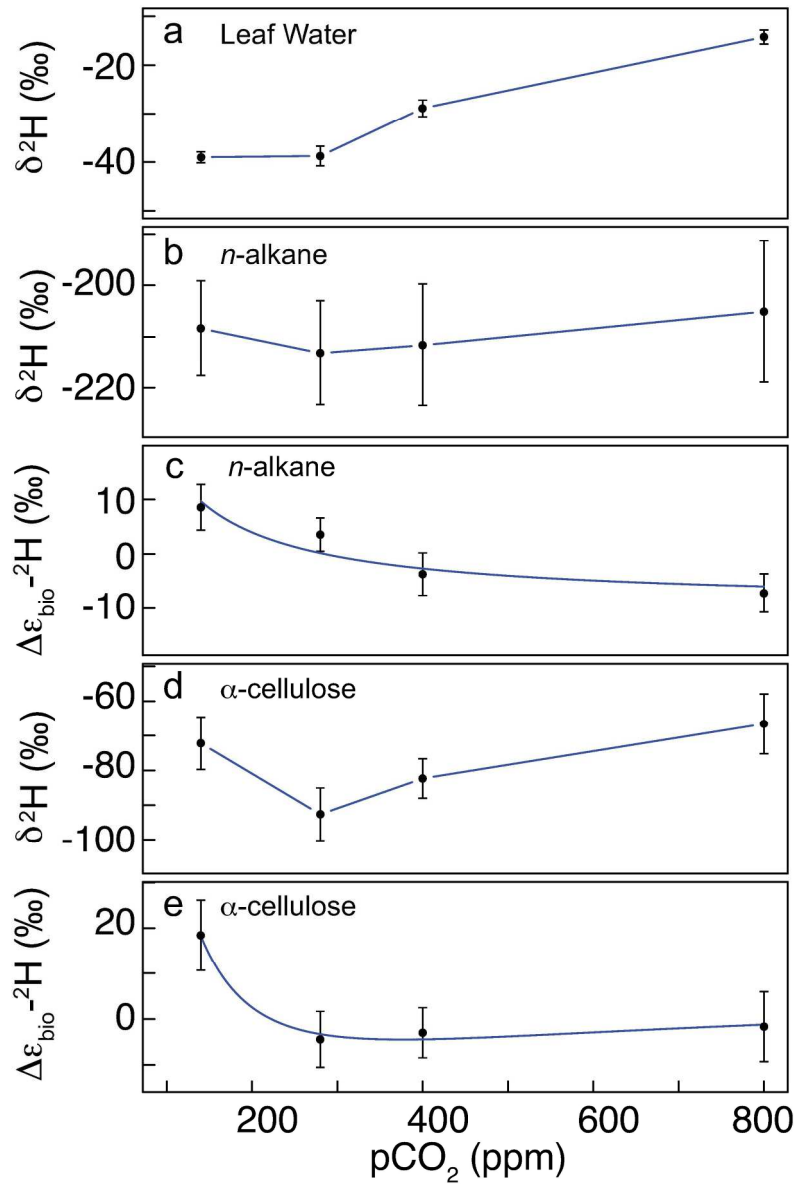


Fig. 2. Leaf water,  $\alpha$ -cellulose, *n*-alkane  $\delta^2\text{H}$  values and  $\Delta^2\text{H}-\epsilon_{\text{bio}}$  for  $\alpha$ -cellulose and *n*-alkanes under different  $\text{pCO}_2$  averaged across all six species. The magnitude of  $^2\text{H}-\epsilon_{\text{bio}}$  can differ largely across different species. To allow the comparison of treatment effects on  $^2\text{H}-\epsilon_{\text{bio}}$  across all six species we standardized the  $^2\text{H}-\epsilon_{\text{bio}}$  response of a species to the  $\text{pCO}_2$  treatment around its overall mean  $^2\text{H}-\epsilon_{\text{bio}}$  in the experiment (i.e.  $\Delta^2\text{H}-\epsilon_{\text{bio}}$ ). Each point corresponds to the averaged values 6 different species ( $n=6$ ) grown in 3 replicates from seeds under the different  $\text{pCO}_2$ . The  $^2\text{H}-\epsilon_{\text{bio}}$  curves for individual species are available of Fig. S1.



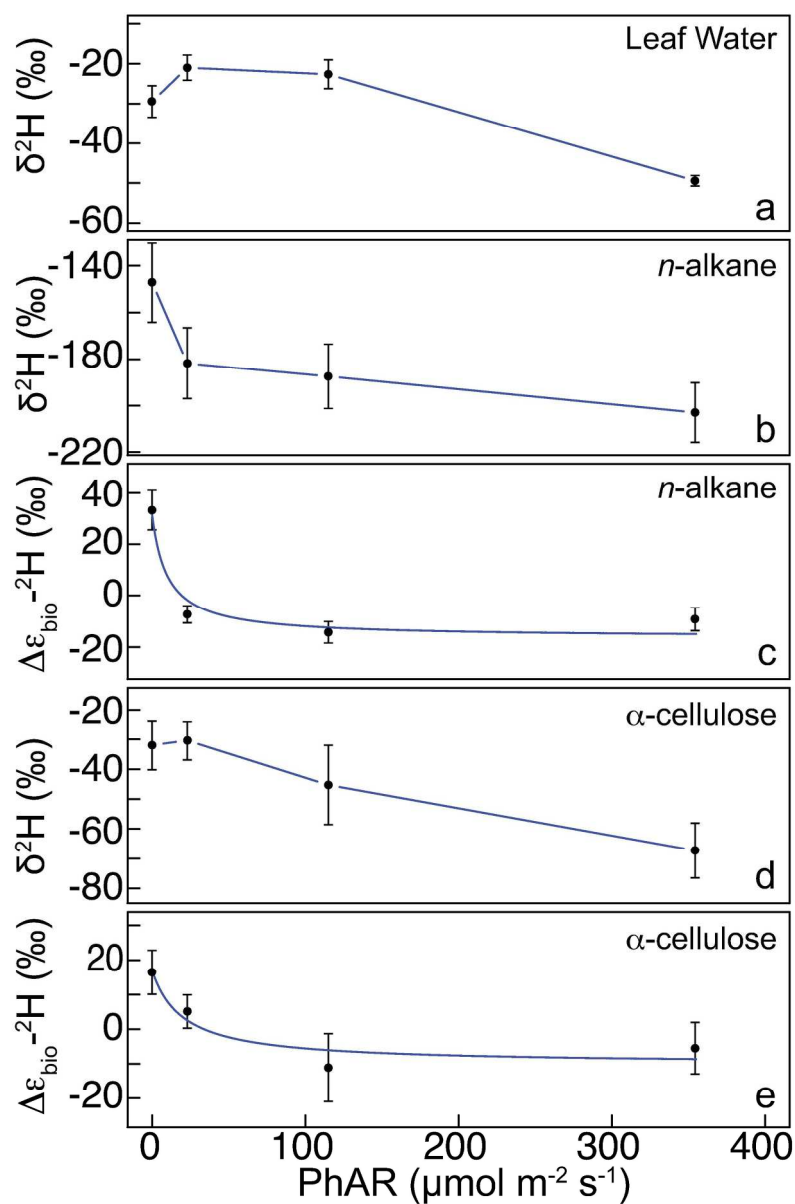


Fig. 3. Leaf water,  $\alpha$ -cellulose, *n*-alkane  $\delta^2\text{H}$  values and the corresponding relative  $^2\text{H}\text{-}\epsilon_{\text{bio}}$  for  $\alpha$ -cellulose and *n*-alkanes under different light intensities (photosynthetic active radiation, PhAR) averaged across all six species. The magnitude of  $^2\text{H}\text{-}\epsilon_{\text{bio}}$  can differ largely across different species. To allow the comparison of treatment effects on  $^2\text{H}\text{-}\epsilon_{\text{bio}}$  across all six species we standardized the  $^2\text{H}\text{-}\epsilon_{\text{bio}}$  response of a species to the light treatment around its overall mean  $^2\text{H}\text{-}\epsilon_{\text{bio}}$  in the experiment (i.e.  $\Delta^2\text{H}\text{-}\epsilon_{\text{bio}}$ ). Each point corresponds to the averaged values 6 different species ( $n=6$ ) grown in 3 replicates from the tuber or roots under the different light intensity. The  $^2\text{H}\text{-}\epsilon_{\text{bio}}$  curves for individual species are available of Fig. S2.

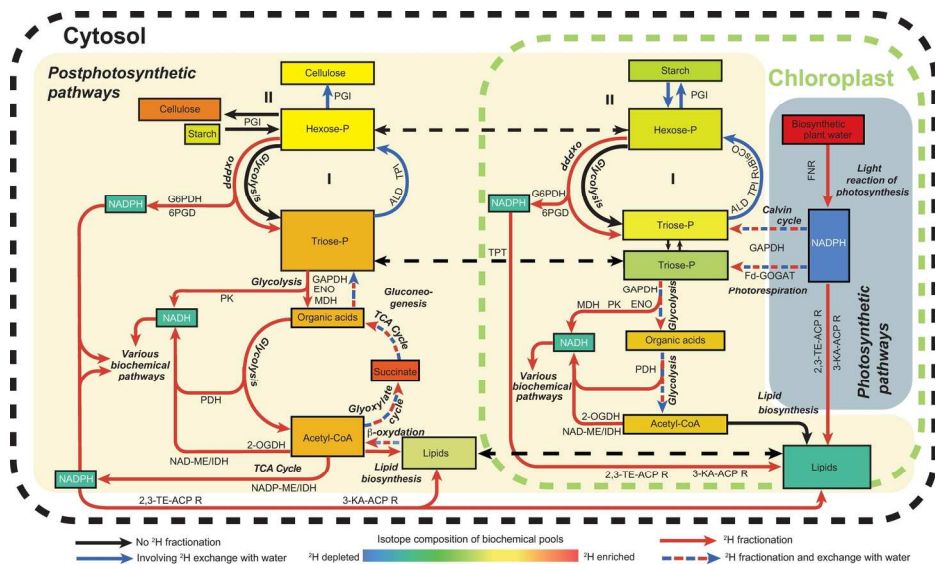


Fig. 4. Schematic view of H flow during processes leading to *n*-alkanes and  $\alpha$ -cellulose  $^2\text{H}\text{-}\epsilon_{\text{bio}}$ . The key enzymes and pathways responsible for H flow are indicated by their following abbreviations and are based on known biochemical pathways (Rose & Rieder, 1958; Rieder & Rose, 1959; Knowles & Albery, 1977; Cheesbrough & Kolattukudy, 1984; Schleucher et al., 1999; Heldt et al., 2005; Augusti et al., 2006; Zhang et al., 2009; Schirmer et al., 2010; Voet & Voet, 2011; Buchanan et al., 2015; Ehlers et al., 2015). The Roman numerals indicate the two main post-photosynthetic biochemical processes that we suggest to be responsible for the general  $^2\text{H}$ -enrichment of plant metabolites under low photosynthetic carbohydrate supply: 2-OGDH, 2-oxoglutarate dehydrogenase; 6PGD, 6-phosphogluconate dehydrogenase; ACP, acyl-carrier-protein; ALD, aldolase; ENO, enolase; Fd-GOGAT, ferredoxin glutamine:oxoglutarate aminotransferase; FNR, ferredoxin-NADP<sup>+</sup> reductase; G6PDH, glucose-6-phosphate dehydrogenase; GAP, glyceraldehyde 3-phosphate; GAPDH, glyceraldehyde 3-phosphate dehydrogenase; IDH, isocitrate dehydrogenase; KA, ketoacyl; ME, malic enzyme; NADP, nicotinamide adenine dinucleotide; NADPH, nicotinamide adenine dinucleotide phosphate; ME, malate dehydrogenase; PDH, pyruvate dehydrogenase; PEP, phosphoenolpyruvate; PGI, phosphoglucose isomerase; PK, pyruvate kinase; oxPPP, oxidative pentose phosphate pathway; TPI, triosephosphate isomerase; TE, trans-enoyl; TPT, triose phosphate translocator; R, reductase; RuBisCO, ribulose-1,5-bisphosphate carboxylase/oxygenase. Succinate dehydrogenase also produced  $\text{FADH}_2$  in the TCA cycle, but is not represented on the scheme.

172x95mm (300 x 300 DPI)

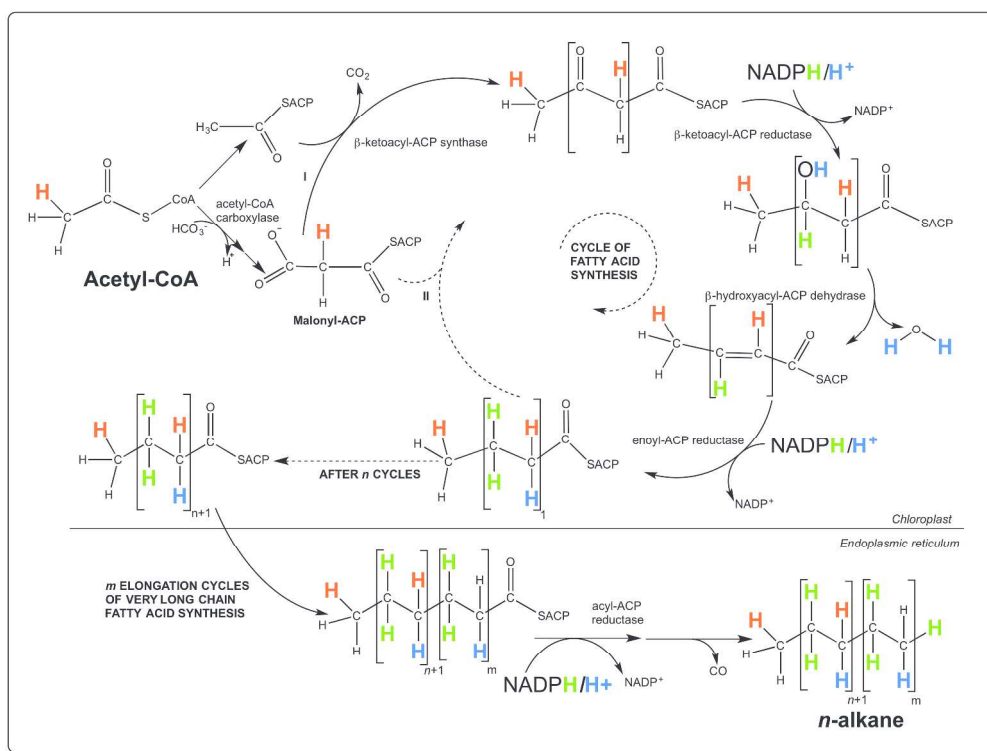


Fig. 5. Simplified view of the biochemical origins of H atoms in *n*-alkane biosynthesis. Black H represent H atoms from the precursor acetyl-CoA. Green H originate from  $\text{NADPH}$  reduced by the light reaction of photosynthesis in the chloroplast and/or by oxPPP and other reactions in the endoplasmic reticulum. Blue H are from H atoms in equilibrium with surrounding water. The fatty acids are generally elongated until 16 or 18 Cs long in the chloroplast and until 32 Cs long in the endoplasmic reticulum; this might also imply different H sourcing (Cheesbrough & Kolattukudy, 1984; Zhang et al., 2009; Schirmer et al., 2010; Buchanan et al., 2015). The red H represent the  $^2\text{H}$ -depleted atoms that can come from the 3-phosphoglycerate produced upon the photosynthetic C oxidation. In a C29-alkane, of 60 H atoms, 28 comes from  $\text{NADPH}$ , 14 from water, 17 from malonyl-ACP (which ultimately derives from acetyl-CoA and pyruvate).

298x223mm (300 x 300 DPI)